Dalton Transactions

PAPER

View Article Online
View Journal | View Issue

Cite this: *Dalton Trans.*, 2014, **43**, 14377

Heterometallic aluminates: alkali metals trapped by an aluminium aryloxide claw†

Mª Teresa Muñoz, Tomás Cuenca* and Marta E. G. Mosquera*

Received 31st March 2014,
Accepted 6th June 2014

DOI: 10.1039/c4dt00952e

www.rsc.org/dalton

A series of heterometallic aluminium–alkali metal species $[AlMMe_2\{2,6\text{-}(MeO)_2C_6H_3O\}_2]_n$ have been isolated for lithium, sodium and potassium. These compounds can be generated by the reaction of $[AlMe_2\{2,6\text{-}(MeO)_2C_6H_3O\}]_2$ with the metallated phenol $[M\{2,6\text{-}(MeO)_2C_6H_3O\}]_n$ or through the reaction of the mixture of $AlMe_3$ and the appropriate alkali metal alkyl base with two equivalents of 2,6-dimethoxyphenol. In the heterometallic species obtained, the $\{AlMe_2\{2,6\text{-}(MeO)_2C_6H_3O\}_2\}^-$ moiety is observed and could be described as a claw which fixes the alkali ion by the phenoxide oxygen atoms while the methoxy groups help to stabilize their coordination sphere. All compounds have been characterized by NMR spectroscopy and X-ray diffraction methods. Catalytic studies reveal that these compounds are active in ring-opening polymerization of L-lactide.

Introduction

Aluminium organometallic compounds are well known for their remarkable structures and unique reactivity.[1] These derivatives participate in many organic transformations such as nucleophilic additions to carbonyl compounds,[2] cross coupling reactions with organic halides,[3] hydro- and carboaluminations to unsaturated species,[4] conjugative addition to Michael acceptors[5] and many others.[6] In addition, they are active in numerous catalytic polymerization processes of a variety of substrates such as olefines,[7] or functionalized monomers like epoxides[8] and cyclic esters.[9] In these processes those species containing Al–O bonds are particularly active.[10]

The reactivity of aluminium organometallics stems either from the acidic character of the metal or from the carbanionic nature of the organic group bonded to it.[11] This dual Lewis character confers great versatility to the chemical behaviour of these compounds. A kind of derivatives in which this multi Lewis character is particularly evident is the group 1 aluminates, where an alkali metal and the aluminium are placed in close proximity.[12]

For these heterometallic systems the presence of two metals of different nature, one very electropositive alkali metal and a p-block metal, could provide valuable synergic effects, so reactivities and selectivities different from the homometallic counterparts can be expected.[13] In fact, the interest in heterometallic "ate" species has increased exponentially since the beginning of the century due to the remarkable reactivity that they have shown.[14] As such, these species have revolutionized the metallating reactions, outperforming traditional single metal metallating agents such as alkyl lithium compounds.[15]

Although "ate" derivatives have been tested in many organic transformations, studies on their ability as polymerization catalysts are scarce.[16] Hence it is of interest to evaluate the activity of aluminate species in such processes, especially considering that aluminium is a key metal in the preparation of active species for catalytic polymerizations.

In this context, our research is oriented to the preparation of aluminium derivatives active in polymerization processes.[17] Particularly we are interested in studying derivatives with functionalized aryloxide groups since the additional functionalities in the ring can influence the structure and reactivity of the species formed.[18,19] Surprisingly there are few studies of functionalized phenols as ligand precursors even though they are cheap, readily available chemicals.

In this study, a phenol bearing donor group in the *ortho* position, 2,6-dimethoxyphenol, has been chosen as the ligand precursor. In our previous investigations we have isolated heterometallic ate species of different nuclearity, $[AlLiMe_3\{2,6\text{-}(MeO)_2C_6H_3O\}]_3$ and $[AlLiMe_2\{2,6\text{-}(MeO)_2C_6H_3O\}_2]_2$, from the reaction of the hexametallic lithium aryloxide cage $[Li\{2,6\text{-}(MeO)_2C_6H_3O\}]_6$ and different aluminium precursors.[19]

We report here the extension of our work to potassium and sodium, using $[AlMe_2\{2,6\text{-}(MeO)_2C_6H_3\}]_2$ (**2**) as the aluminium precursor. These studies have allowed us to isolate the metal-

---

Departamento de Química Orgánica y Química Inorgánica, Universidad de Alcalá, Campus Universitario, E-28871 Alcalá de Henares, Spain.
E-mail: martaeg.mosquera@uah.es; Fax: +34-918854683; Tel: +34-918854779

† Electronic supplementary information (ESI) available: DOSY experiments for **3b** and **3c**, ^1H NMR data for **2** and $[ZpCp_2Cl(OAr)]$, a scaterogram of Al–O distances and dihedral angles between a Al_2O_2 plane and a phenyl ring for $(AlOAr)_2$ derivatives. CCDC 993198–993200. For ESI and crystallographic data in CIF or other electronic format see DOI: 10.1039/c4dt00952e

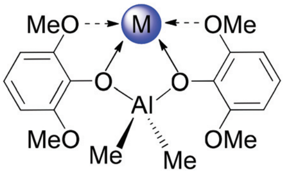

Fig. 1 Aluminium phenoxide claw, M = Li, Na, K.

lated phenols $[M\{2,6\text{-}(MeO)_2C_6H_3\}]_n$ (M = Na (**1b**), K (**1c**)) and the two new heterometallic ate compounds $[AlMMe_2\{2,6\text{-}(MeO)_2C_6H_3O\}_2]_n$ (M = Na (**3b**), K (**3c**)). Interestingly, compound **3c** is the first potassium–aluminium derivative with aryloxide ligands bridging the metals. The structure of the heterometallic derivatives **3b** and **3c** was determined in the solid state and both show the structural motif $\{AlMe_2(2,6\text{-}(MeO)_2C_6H_3O)_2\}^-$, analogous to the one present in the lithium species previously described by our group.[19] This fragment acts as a kind of claw that can grasp alkali metals of very different sizes such as lithium and potassium, without changing substantially its structural parameters (Fig. 1). The solid state structure of the species $[AlMe_2\{2,6\text{-}(MeO)_2C_6H_3\}]_2$ (**2**)[19] previously reported by us is also described.

Experimental section

General considerations

All manipulations were carried out under an inert atmosphere of argon using standard Schlenk and glovebox techniques. All solvents were rigorously dried prior to use following standard methods. NMR spectra were recorded at 400.13 (^1H) and 100.62 (^{13}C) MHz on a Bruker AV400. Chemical shifts (δ) are given in ppm using C_6D_6 and THF-d_8 as the solvent. ^1H and ^{13}C resonances were measured relative to solvent peaks considering TMS $\delta = 0$ ppm. Elemental analyses were obtained on a Perkin-Elmer Series II 2400 CHNS/O analyzer. Molecular weights of polymers were determined by gel permeation chromatography (GPC) in a Varian HPL apparatus in THF at room temperature calibrated with respect to polystyrene standards and corrected with a factor of 0.58. L-Lactide was purchased from Aldrich and then purified by recrystallization from toluene and sublimation under vacuum. All reagents were commercially obtained and used without further purification. Benzyl sodium,[20] benzyl potassium[20] and $[AlMe_2\{2,6\text{-}(MeO)_2C_6H_3\}]_2$[19] were prepared according to reported methods.

Synthesis of $[Na\{2,6\text{-}(MeO)_2C_6H_3O\}]_n$ (1b). To a solution of benzyl sodium (0.37 g, 3.21 mmol) in 10 mL of toluene, a solution of 2,6-dimethoxyphenol (0.50 g, 3.21 mmol) in 10 mL of toluene was added at −78 °C. The mixture was stirred for 10 min at low temperature and then allowed to reach room temperature, and then again stirred for 2 hours, and the precipitation of a white solid was observed. Yield: 53% (0.30 g, 1.70 mmol). ^1H NMR (C_6D_6): δ 3.24 (s, 6H, O*CH*$_3$), 6.51 (m, 3H, OAr-*H*). ^{13}C (C_6D_6): δ 55.76 (s, O*C*H$_3$), 105.93 (s, *p*-OAr-H), 108.64 (*m*-OAr-H), 150.34 (s, *o*-OAr), 151.16 (d, i-OAr). Anal. Calcd (%) for $NaC_8H_9O_3$ (176.15 g mol^{-1}) C, 54.50; H, 5.11. Found: C, 53.81; H, 5.05.

Synthesis of $[K\{2,6\text{-}(MeO)_2C_6H_3O\}]_n$ (1c). To a solution of benzyl potassium (0.418 g, 3.21 mmol) in 10 mL of toluene, a solution of 2,6-dimethoxyphenol (0.50 g, 3.21 mmol) in 10 mL of toluene was added at −78 °C. The suspension changed from red to white colour. The mixture was stirred for 10 min at low temperature and then allowed to reach room temperature, and then again stirred for 3 hours, and the precipitation of a white solid was observed. Yield: 54% (0.33 g, 1.73 mmol). ^1H NMR (C_6D_6): δ 3.13 (s, 6H, O*CH*$_3$), 6.41 (m, 3H, OAr-*H*). ^{13}C (C_6D_6): δ 54.54 (s, O*C*H$_3$), 104.22 (s, *m*-OAr-H), 109.38 (s, *p*-OAr-H), 150.98 (s, OAr). Anal. Calcd (%) for $KC_8H_9O_3.0.1C_7H_8$ (201.47 g mol^{-1}) C, 51.87; H, 4.90. Found: C, 52.71; H, 4.45.

Synthesis of $[AlNaMe_2\{2,6\text{-}(MeO)_2C_6H_3O\}_2]_2$ (3b). To a mix of 0.10 g (0.568 mmol) of **1b** and 0.12 g (0.284 mmol) of $[AlMe_2\{2,6\text{-}(MeO)_2C_6H_3\}]_2$ was added 10 mL of toluene at −78 °C. The mixture was stirred for 10 min at low temperature and then allowed to reach room temperature, and the precipitation of a white solid was observed. The suspension was stirred for 2 hours at room temperature. The solid was dissolved after a brief reflux. Storage of the solution at room temperature for a day allowed the formation of white crystals of compound **3b**. Yield: 60% (0.13 g, 0.34 mmol). ^1H NMR (C_6D_6): δ −0.49 (s, 3H, Al*CH*$_3$), 3.40 (s, 6H, O*CH*$_3$), 6.29 (d, 2H, $^3J_{HH}$ = 8 Hz, *m*-OAr-*H*), 6.56 (t, 1H, $^3J_{HH}$ = 8 Hz, *p*-OAr-*H*). ^{13}C (C_6D_6): δ −-10.33 (s, Al*C*H$_3$), 55.72 (t, O*C*H$_3$), 105.60 (t, *m*-OAr-H), 116.33 (s, *p*-OAr-H), 140.44 (s, *o*-OAr), 150.57 (s, i-OAr). Anal. Calcd (%) for $Na_2Al_2C_{36}H_{48}O_{12}$ (772.58 g mol^{-1}) C, 55.96; H, 6.26. Found: C, 55.71; H, 6.59.

Synthesis of $[AlKMe_2\{2,6\text{-}(MeO)_2C_6H_3O\}_2]_n$ (3c). A solution of 2,6-dimethoxyphenol (0.50 g, 3.21 mmol) in toluene (10 mL) was added to 0.42 g (3.21 mmol) of KBz in 10 mL of toluene at −78 °C, and the mixture was stirred for 10 minutes. Then the solution was allowed to reach room temperature. After stirring for 2 hours, a grey solution with solids was formed. 0.68 g (1.60 mmol) of $[AlMe_2\{2,6\text{-}(MeO)_2C_6H_3O\}]_2$ heated to a brief reflux in 20 mL of toluene was added to the suspension and stirred for 10 minutes. When the reaction mixture reached room temperature the white solid formed was dissolved by heating while 25 mL of THF was added, giving a pale yellow solution. After one day of storage at room temperature, white crystals of compound **3c** were observed. Yield: 52% (0.68 g, 1.68 mmol). ^1H NMR (THF-d_8): δ −1.10 (s, 3H, Al*CH*$_3$), 3.71 (s, 6H, O*CH*$_3$), 6.38 (m, 1H, *p*-OAr-*H*), 6.45 (m, 2H, *m*-OAr-*H*). ^1H NMR (C_6D_6): δ −0.50 (s, 3H, Al*CH*$_3$), 3.35 (s, 6H, O*CH*$_3$), 6.30 (m, 2H, *m*-OAr-*H*), 6.48 (m, 1H, *p*-OAr-*H*). ^{13}C (C_6D_6): δ −9.00 (s, Al*C*H$_3$), 55.36 (s, O*C*H$_3$), 104.17 (s, *m*-OAr-H), 105.64 (s, *p*-OAr-H), 138.10 (s, *o*-OAr), 151.23 (s, i-OAr). Anal. Calcd (%) for $KAlC_{18}H_{24}O_6$ (402.46 g mol^{-1}) C, 53.72; H, 6.01. Found: C, 52.93; H, 5.51.

Polymerization of L-lactide

In a glovebox, a Schlenk flask was charged with 26 μmol of the desired complex and 26 μmol of benzyl alcohol. 2.5 mL of dry toluene was added. This solution was added to 2.6 mmol (373 mg) of L-lactide dissolved in 2.5 mL of dry toluene and the mixture was heated in an oil bath at 125 °C. Small portions were removed with a pipette to determine the conversion by ^{1}H NMR. After 5 h, polymerization was quenched with hexane, then it was purified with dichloromethane and, finally, the polymer was precipitated with an excess of hexane. The white solid was filtrated and dried under vacuum to constant weight.

Circular dichroism (CD)

Measurements were performed using a JASCO-715 spectropolarimeter. Recorded spectra were the average of 2 scans taken at the speed of 50 nm min^{-1} with a 0.125 s time response. The sensitivity and resolution were fixed at 20 mdeg and 0.5 nm respectively. Measurements were carried out in 1 cm path quartz cells at 25 °C. The sample was measured in toluene at several concentrations. No CD spectrum was obtained for any of the solutions whatever the concentration was. Results show the absence of any chirality in solution.

Structure determination of compounds 2, 3b and 3c·C_4H_8O

Details of the X-ray experiment, data reduction, and final structure refinement calculations are summarized in Table 1. Suitable single crystals of **2**, **3b** and **3c·C_4H_8O** for the X-ray diffraction study were selected. Data collection was performed at 200(2) K, with the crystals covered with perfluorinated ether oil. The crystals were mounted on a Bruker-Nonius Kappa CCD single crystal diffractometer equipped with a graphite-monochromated Mo-Kα radiation (λ = 0.71073 Å). Multiscan[21] absorption correction procedures were applied to the data. The structures were solved using the WINGX package,[22] by direct methods (SHELXS-97) and refined using full-matrix least-squares against F^2 (SHELXL-97).[23] All non-hydrogen atoms were anisotropically refined. Hydrogen atoms were geometrically placed and left riding on their parent atoms. A disordered THF molecule per asymmetric unit of **3c** is present in the unit cell; this solvent molecule was found in the difference Fourier map but was very disordered and it was not possible to get a chemically sensible model for it, so the Squeeze procedure[24] was used to remove its contribution to the structure factors. Full-matrix least-squares refinements were carried out by minimizing $\sum w(F_o^2 - F_c^2)^2$ with the SHELXL-97 weighting scheme and stopped at shift/err < 0.001. The final residual electron density maps showed no remarkable features.

Crystallographic data (excluding structure factors) for the structures reported in this paper have been deposited with the Cambridge Crystallographic Data Centre as supplementary publication no. CCDC-993198 [**2**], CCDC-993199 [**3b**] and CCDC-993200 [**3c·C_4H_8O**].

Results and discussion

The approach to achieve the formation of heterometallic species may be oriented in two ways; one would imply the initial reaction of 2,6-dimethoxyphenol with the alkali metal alkyl base MR and then the treatment of the metallated phenol with the aluminium precursor $[AlMe_2\{2,6\text{-}(MeO)_2C_6H_3O\}]_2$ (**2**). In the other synthetic approach the initial step would be to generate an alkali metal–aluminium heterometallic species by mixing $AlMe_3$ and MR that would then

Table 1 Crystallographic data for **2**, **3b** and **3c**·C_4H_8O

	2	3b	3c·C_4H_8O
Formula	$C_{20}H_{30}Al_2O_6$	$C_{36}H_{48}Al_2Na_2O_{12}$	$C_{18}H_{24}AlKO_6{\cdot}C_4H_8O$
FW	420.40	772.68	474.56
Color/habit	Colourless/block	Colourless/block	Colourless/block
Cryst dimensions (mm^3)	0.38 0.25 0.21	0.45 0.43 0.28	0.49 0.46 0.37
Cryst Syst	Orthorhombic	Orthorhombic	Monoclinic
Space group	*Pbca*	$P2_12_12$	$P2_1/c$
a (Å)	15.3154(12)	13.7778(16)	12.4801(13)
b (Å)	9.5003(8)	14.062(3)	7.311(2)
c (Å)	16.2703(17)	10.594(3)	25.671(7)
β (°)	90	90	92.860(17)
V (Å^3)	2367.3(4)	2052.4(8)	2339.5(9)
Z	4	2	4
T (K)	200	200	200
ρ_{calcd} (g cm^{-3})	1.180	1.250	1.347
μ (mm^{-1})	0.152	0.149	0.304
F(000)	896	816	1008
θ range (°)	3.42–26.60	3.25–27.51	3.18–27.50
No. of rflns collected	36 478	35 554	42 907
No. of indep rflns/R_{int}	2474/0.0979	4697/0.0470	5351/0.0518
No. of data/restraints/params	2474/0/127	4697/0/236	5351/0/235
R_1/wR_2 ($I > 2\sigma(I)$)[a]	0.0523/0.1421	0.0505/0.1392	0.0835/0.2146
R_1/wR_2 (all data)[a]	0.1009/0.1636	0.0838/0.1577	0.1083/0.2260
Flack parameter		0.0(3)	
GOF (on F^2)[a]	1.036	1.032	1.103
Diff. peak/hole (e Å^{-3})	0.255/−0.194	0.325/−0.503	0.676/−0.767

[a] $R_1 = \sum(||F_o| - |F_c||)/\sum|F_o|$; $wR_2 = \{\sum[w(F_o^2 - F_c^2)^2]/\sum[w(F_o^2)^2]\}^{1/2}$; GOF $= \{\sum[w(F_o^2 - F_c^2)^2]/(n - p)\}^{1/2}$.

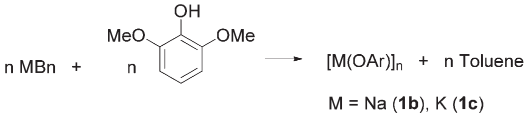

Scheme 1 Synthesis of **1**.

react with the right stoichiometric amount of 2,6-dimethoxyphenol.

Starting with the first strategy, in order to prepare the sodium and potassium derivatives $[M(OAr)]_n$, 2,6-dimethoxyphenol was reacted with benzyl sodium and benzyl potassium, giving the species $[M\{2,6\text{-}(MeO)_2C_6H_3O\}]_n$ (M = Na (**1b**), K (**1c**)) (see Scheme 1).

Compounds **1b** and **1c** are air sensitive and should be stored under argon. They were characterized by analytical and spectroscopic methods. The formation of **1** was confirmed by the disappearance of the signal for the alcohol group in the ^{1}H NMR spectra, where similar resonances are observed for **1b–1c** in comparison to the previously reported lithium derivative $[Li\{2,6\text{-}(MeO)_2C_6H_3O\}]_6$.[19] As such, we observe one singlet at 3.24 (**1b**) and 3.13 (**1c**) ppm for the methoxy group hydrogen atoms, being at 3.16 ppm for the lithium derivative. The resonances for the aromatic ring also appear at close shift values for these compounds, a multiplet at 6.51 (**1b**) and 6.14 (**1c**) ppm, being slightly different in the lithium case, which shows a doublet at 6.48 ppm and a triplet at 6.56 ppm for *meta* and *para* protons respectively.

The reaction of compounds **1** and $[AlMe_2\{2,6\text{-}(MeO)_2C_6H_3O\}]_2$ (**2**) led to the formation of the heterometallic derivatives **3b** and **3c** that were isolated as colourless crystals (see Scheme 2). The potassium species **3c** is barely soluble in toluene so it was necessary to use a donor solvent such as THF to dissolve it and achieve the formation of crystals.

When we perform the synthesis of the heterometallic species using the second strategy, that is, by mixing initially the metallic precursors $AlMe_3$ and MR and then adding two equivalents of 2,6-dimethoxyphenol, the corresponding heterometallic compounds **3** were also generated, although the yields are lower and the formation of other species is observed in the NMR spectra.

Compounds **3** are air sensitive and should be stored under argon, but for short periods of time remain unchanged in air. They were characterized in solution by multinuclear NMR spectroscopy. In the ^{1}H NMR spectra in C_6D_6, $[AlLiMe_2\{2,6\text{-}(MeO)_2C_6H_3O\}_2]_2$ and compounds **3** show a resonance for the methyl groups bound to aluminium at similar values (δ *ca.* −0.50), indicating an analogous electronic environment for those methyl groups in the three compounds. The other hydrogen atoms in the structure appear also at similar shifts for the three derivatives (δ 3.35–3.40 (OMe range), 6.23–6.30 (*m*-OAr-*H* range) and 6.48–6.56 (*p*-OAr-*H* range)). These data suggest that the methyl groups have the same acidic character and the different alkali metals have a little effect on the shielding of those protons. However, there is an important change in comparison to the precursor $[AlMe_2\{2,6\text{-}(MeO)_2C_6H_3O\}]_2$ (**2**), in that, the signal for the methyl group bonded to the aluminium moves significantly to higher field values, from −0.27 ppm in **2** to −0.50 ppm in **3** signifying a more shielded environment for the methyl groups in the aluminates.

The nuclearities in the solid state for compounds **3** were determined by single-crystal X-ray diffraction studies since appropriate crystals were isolated. Also, for comparison purposes the study of the structure of the aluminium precursor $[AlMe_2\{2,6\text{-}(MeO)_2C_6H_3O\}]_2$ (**2**) was also performed.

As shown in Fig. 2, compound **2** is a dinuclear derivative where the aryloxide group acts as a bridging ligand. In this compound, the aluminium centres show a typical tetrahedral environment, being bonded to two aryloxide ligands and two methyl groups. There is also a non-covalent interaction between the oxygen atoms from the MeO moieties and the aluminium, Al⋯OMe 2.59 Å and 2.54 Å, giving a pseudo-octahedral environment for the metal. The central core Al_2O_2 and the two phenyl rings are co-planar, and this disposition is probably affected by the presence of these Al⋯OMe interactions. In fact, a CSD (Cambridge Structural Database) search[25] showed that the most frequent arrangement for derivatives bearing the fragment $(AlOAr)_2$ is when the central Al_2O_2 plane and the phenyl rings are placed at an angle bigger than 40°. For those cases where the angle is close to planarity, in the vast majority of the compounds there is a substituent in the *ortho* position that establishes an interaction with the

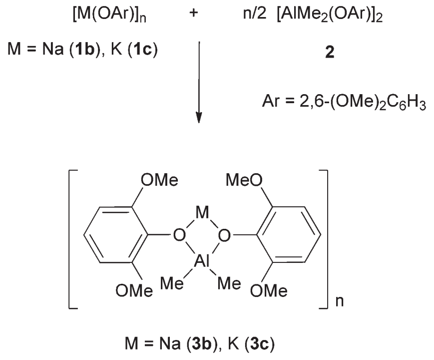

Scheme 2 Synthesis of **3**.

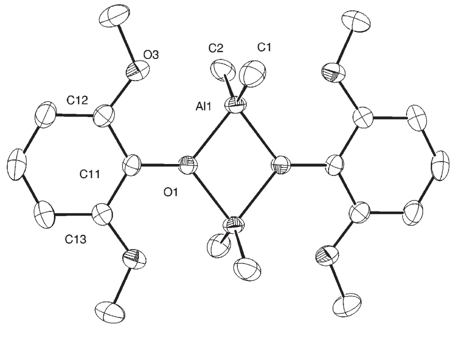

Fig. 2 ORTEP plot of **2** showing thermal ellipsoid plots (30% probability).

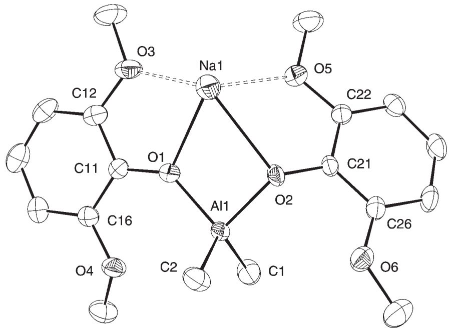

Fig. 3 ORTEP plot of **3b** asymmetric unit showing thermal ellipsoid plots (30% probability).

metal directing this co-planar disposition, as in **2**. For these kinds of $(AlOAr)_2$ derivatives a clear tendency in the Al–O distance is also observed, being shorter for those compounds with a coplanar arrangement of the Al_2O_2 plane and the phenyl rings (see ESI†).

In Fig. 3, an ORTEP view for the asymmetric unit of **3b** along with the atom-labelling schemes is shown. In this unit, the presence of one aluminium atom and one sodium atom bridged by two phenoxide groups is observed. The aluminium center completes its coordination sphere with two methyl groups. The sodium atom is bonded to a $\{AlMe_2\{2,6\text{-}(MeO)_2C_6H_3O\}_2\}^-$ fragment that grabs the alkali ion.

This $\{AlMe_2(2,6\text{-}(MeO)_2C_6H_3O)_2\}^-$ moiety is also present in compound **2**, although in this case it would be binding a $\{Al(CH_3)_2\}^+$ fragment. When comparing the bond distances and angles in this fragment for **2** and **3b**, a shortening of the Al–O bonds lengths and an increase of the O–Al–O angle are observed for the heterometallic derivative (Table 2). However, the Al–C distances do not change significantly.

When a **3b** asymmetric unit is grown, a tetrametallic Na_2Al_2 derivative is revealed (see Fig. 4a). In this structure the two aryloxide oxygen atoms, O1 and O2, are bridging the aluminium and sodium atoms composing two four-membered rings that are attached to the central Na_2O_2 core by sharing the Na1–O2 edge. The Na–O distances in this central cycle are quite different from each other (2.272(4) and 2.466(4) Å). The disposition of the aryl groups projected above and below the Na_2O_2 plane prevents the cycles from stacking[26] and the three four-membered rings associate laterally in a cradle disposition.

In **3b** the sodium atoms are pentacoordinated, bonded to three aryloxide groups and two methoxy moieties. The interactions observed between the sodium and the methoxy groups are asymmetric, Na···OMe 2.310 and 2.903 Å, and help to stabilise the coordination sphere of the alkali metal. In a similar way as in **2**, the close disposition of two methoxy groups in relation to the aluminium atoms suggests the presence of weak interactions Al1···O3 and Al1···O4 giving a hexacoordinated environment for the aluminium. This structure is analogous to the one observed for the lithium counterpart $[AlLiMe_2\{2,6\text{-}(MeO)_2C_6H_3O\}_2]_2$.[19] However, in this case the central rings are bigger, as expected due to the higher ionic radius of sodium in comparison to lithium.[27]

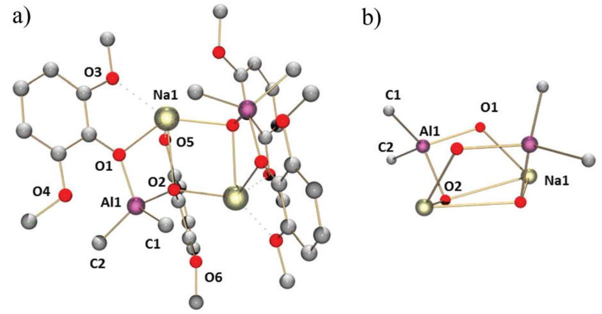

Fig. 4 (a) Ball and stick plot of compound **3b**. (b) Central core.

Table 2 Selected bond lengths (Å) and angles (°) for **2**, $[AlLiMe_2\{2,6\text{-}(MeO)_2C_6H_3O\}_2]_2$, **3b** and **3c**[a]

Bond lengths					
	2		[AlLi][19]	**3b**	**3c**
Al1–O1	1.890(2)	Al1–O1	1.852(1)	1.798(2)	1.810(3)
Al(1)–O(1)#1	1.898(2)	Al1–O2	1.799(2)	1.833(2)	1.819(3)
O1–C11	1.368(3)	O1–C11	1.359(2)	1.314(4)	1.335(4)
C11–C12	1.382(4)	C11–C12	1.390(3)	1.405(4)	1.388(6)
C12–O3	1.358(3)	C12–O3	1.372(3)	1.372(4)	1.379(5)
		O2–C21	1.346(2)	1.351(3)	1.341(4)
C11–C13	1.388(4)	C21–C22	1.395(3)	1.385(4)	1.385(6)
C13–O2	1.359(3)	C22–O5	1.385(3)	1.386(4)	1.380(5)
Al1–C1	1.956(3)	Al1–C1	1.960(3)	1.970(3)	1.945(5)
Al1–C2	1.945(3)	Al1–C2	1.950(2)	1.963(4)	1.945(5)
Angles					
O1–Al1–O#1	76.25(9)	O1–Al1–O2	86.93(7)	89.06(10)	86.39(13)
O1–C11–C12	119.9(2)	O1–C11–C12	118.44(19)	120.3(3)	119.3(3)
C11–C12–O3	113.7(2)	C11–C12–O3	113.45(18)	114.1(3)	115.2(3)
O1–C11–C13	120.6(2)	O2–C21–C22	120.80(19)	120.8(3)	119.2(4)
C11–C13–O2	114.0(2)	C21–C22–O5	114.49(18)	115.0(3)	114.5(4)

[a] Symmetry transformations: #1 $-x + 1, -y, -z + 1$.

Another noteworthy difference is that **3b** crystallises in a chiral space group and it is enantiomerically pure. Considering that none of the reactants were chiral, the chirality must come from the central core conformation. As depicted in Fig. 4b, the three rings that compose the central core are arranged helicoidally as a dextro rotatory helix. In solution no chirality is observed, as shown by a circular dichroism study. In order to gain further insight into the structure of **3b** in solution, diffusion-ordered spectroscopy (DOSY) NMR experiments were carried out. Following the methodology applied by several groups,[28] we used three reference compounds and plotted the diffusion coefficients logarithm in relation to the logarithm of the molecular weights (see ESI†). The correlation points towards a formulation [$AlNaMe_2\{2,6\text{-}(MeO)_2C_6H_3O\}_2$] solvated with one solvent molecule. This result will be in agreement with the lack of chirality in solution since it indicates that the central core Na_2O_2 is not present when dissolved.

The structure in the solid state for compound **3c** shows the same asymmetric unit as **3b** where the potassium is again bonded to a $\{AlMe_2\{2,6\text{-}(MeO)_2C_6H_3O\}_2\}^-$ fragment (Fig. 5d and 6d). However, in this case, there is a striking difference due to the bigger size of potassium[27] and, as shown in Fig. 6d, the metal stacks out leaving the moiety $\{AlMe_2\{2,6\text{-}(MeO)_2C_6H_3O\}_2\}^-$ nearly coplanar and with a symmetric coordination to the alkali metal. As such, the dihedral angles between the central AlO_2 core and the phenyl rings are 14.32° and 15.14°, the Al⋯OMe distances being 2.819 Å and 2.869 Å, respectively. For the sodium species **3b**, the coordination of the alkali metal to the aryloxide fragment distorts this arrangement and only one phenyl ring is coplanar with the AlO_2 core (distance Al⋯OMe 2.836 Å), the dihedral angle to the other aromatic ring being 42.51°, which places the OMe group further apart from the aluminium (distance Al⋯OMe 3.263 Å). For the lithium compound this asymmetry is more evident and the dihedral angles between the central core AlO_2 and the aromatic rings are 12.37° and 50.17°, the Al⋯OMe distances being 2.838 Å and 3.255 Å, respectively.

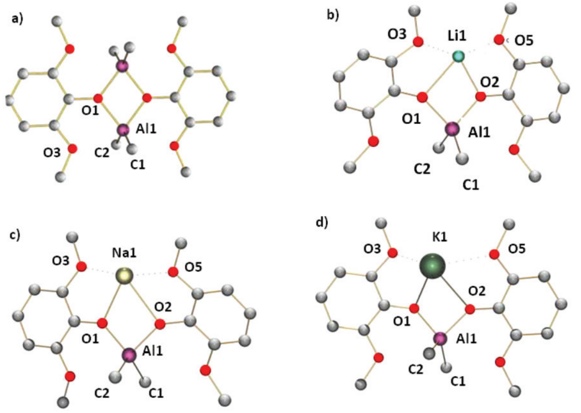

Fig. 5 Ball and stick model for (a) molecular structure of **2**. (b–d) Asymmetric units for [$AlLiMe_2\{2,6\text{-}(MeO)_2C_6H_3O\}_2]_2$, **3b** and **3c** respectively.

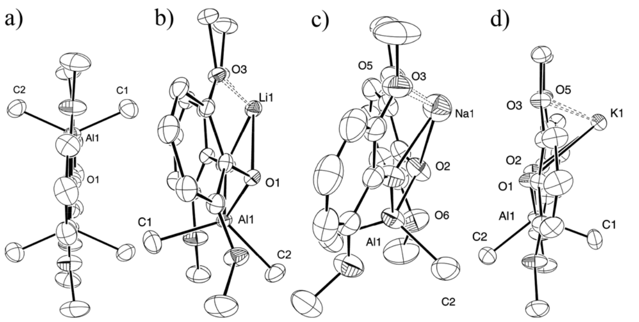

Fig. 6 ORTEP plot showing thermal ellipsoid plots (30% probability) of (a) molecular structure of **2**. (b–d) Asymmetric units for [$AlLiMe_2\{2,6\text{-}(MeO)_2C_6H_3O\}_2]_2$, **3b** and **3c** respectively.

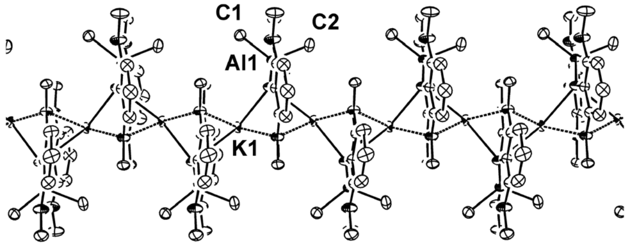

Fig. 7 ORTEP plot of **3c** showing the chain along the *a*-axis (thermal ellipsoid plots 30% probability).

In **3c** the disposition of the aromatic rings' substituents being nearly coplanar to the central core allows the stacking of the units, and instead of the formation of a discrete cradle core, the units pile along the *a*-axis, generating a polymeric structure where the potassium atoms act as the connecting nexus (Fig. 7) of the $\{AlMe_2\{2,6\text{-}(MeO)_2C_6H_3O\}_2\}^-$ fragments that place themselves in alternating positions above and below the potassium chain. The K⋯K distance is 3.6673 Å, shorter than in potassium metal (4.54 Å) and much smaller than double the van der Waals radius of potassium (r_{vdW} = 2.75 Å).[29] Actually, this distance is quite short for a polymeric potassium structure being more often observed in dinuclear derivatives.[30]

As in the aluminium–lithium and aluminium–sodium derivatives, the presence of methoxy groups in the *ortho* position seems to have a decisive effect on the stabilization of the alkali metals through the interactions between the oxygen and these metals. As such, potassium atoms show an octacoordinated arrangement with four bonds shared with phenoxide oxygen atoms and four with methoxy groups (Fig. 8 and 9). This behaviour is different for lithium and sodium species, which show a pentacoordinated arrangement and can be attributed to potassium's bigger size. All the K–O distances in the compound are very similar, either from the bonds to the phenoxide groups, 2.921(4) and 2.939(4) Å, or from the methoxy groups, 2.917(4) and 2.971(4) Å.

All these interactions saturate the coordination sphere of the potassium atom and, although the crystallization took place in the presence of a donor solvent such as THF, no coordinated solvent molecules are present. The structure of this

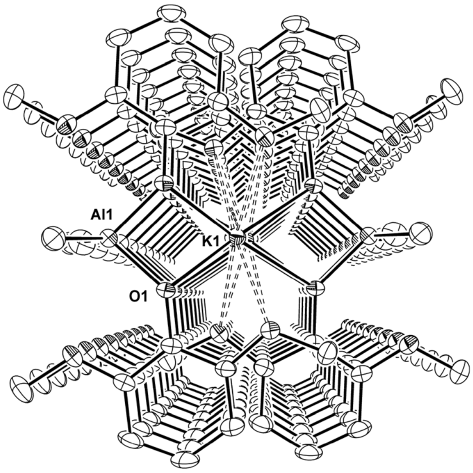

Fig. 8 ORTEP plot of **3c** along the *b*-axis (thermal ellipsoid plots 30% probability).

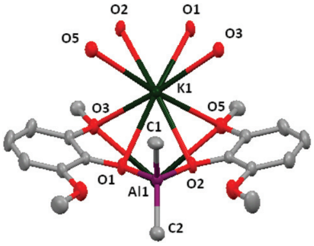

Fig. 9 Potassium coordination sphere in **3c**.

derivative was also analysed in solution by a diffusion-ordered spectroscopy (DOSY) NMR experiment in thf-d_8. In this medium the results indicate the presence of the heterobimetallic species $[AlKMe_2\{2,6\text{-}(MeO)_2C_6H_3O\}_2]$.

According to a search in the CSD, heterometallic aluminium potassium derivatives are not very numerous; those with a K–O–Al fragment being scarce.[31] In particular, compound **3c** is the first potassium–aluminium derivative where the metals are connected by aryloxide bridges.

In conclusion, in the series of compounds $[AlMMe_2\{2,6\text{-}(MeO)_2C_6H_3O\}_2]_2$ (M = Li, Na (**3b**), K (**3c**)) the asymmetric units are isostructural. In them, the alkali metals are chelated by a $\{AlMe_2(2,6\text{-}(MeO)_2C_6H_3O)_2\}^-$ moiety. For the three compounds, bond distances and angles within this fragment are very similar (Al–O distances, 1.798(2)–1.852(1) Å range; C–O distances 1.314(4)–1.359(2) Å range; O–Al–O angles 86.39(13)–89.06(10)° range) (Table 2). The main changes amongst the three are the modification of the dihedral angles between the phenyl groups and the AlO_2 central core to accommodate the different sizes of the alkali ion. Hence, in these structures it can be considered that the phenoxide groups bind to aluminium until coordinative saturation, giving the $\{AlMe_2(2,6\text{-}(MeO)_2C_6H_3O)_2\}^-$ moiety. This anion satisfies the coordinative needs of the approaching alkali metal cation and can be described as a claw which fixes the alkali metals to the framework by the phenoxide oxygen atoms while the methoxy groups help to stabilize the coordination sphere of the alkali metals. These bonding features, where the $Al\text{–}O_{phenoxide}$ bonds show an anchoring nature that provides the framework for the structure, while the alkali metals attach to it *via* ancillary bonds, are in good agreement with the well-established concept of anchoring/ancillary bonding in heterobimetallic chemistry.[32]

Reactivity studies

The reactivity of the $[AlMMe_2\{2,6\text{-}(MeO)_2C_6H_3O\}_2]_2$ (M = Li, Na (**3b**), K (**3c**)) compounds towards $[ZpCp_2Cl_2]$ was analysed. When the reactions for the three compounds were monitored by ^1H NMR spectroscopy, the apparition of two sets of resonances is observed. One group of signals at δ: −0.27 (s, 6H), 3.38 (s, 6H), 6.24 (d, 2H, $^3J_{HH}$ = 8 Hz) and 6.65 (t, 1H, $^3J_{HH}$ = 8 Hz) evidences the generation of derivative **2** in the reaction. The other set of signals at δ: 6.72 (t, 1H, $^3J_{HH}$ = 8 Hz), 6.40 (d, 2H, $^3J_{HH}$ = 8 Hz), 6.19 (s, 10H) and 3.45 (s, 6H) corresponds to the compound $[ZpCp_2Cl(OAr)]$ indicating that the substitution of a Cl ligand for an aryloxide ligand has taken place. A clear tendency of reactivity is observed, as such, after one day, the reaction had evolved to a greater extent for **3c** than for the sodium and lithium counterparts (see ESI† for NMR spectra). This behaviour indicates that the reactivity of these heterometallic species $[AlMMe_2\{2,6\text{-}(MeO)_2C_6H_3O\}_2]_n$ is highly influenced by the alkali metal and the ligand coordinated to it is transferred to the zirconium center, while the aluminum methyl groups remain unreactive.

Initial studies of the conduct of these derivatives in polymerization processes show that they are active in the ROP of L-lactide. We performed the experiments with a 100 : 1 monomer–initiator ratio in toluene, at 125 °C, using BnOH as the initiator and $[AlMMe_2\{2,6\text{-}(MeO)_2C_6H_3O\}_2]_2$ (M = Li, Na (**3b**), K (**3c**)) as catalysts. For comparison purposes, the activity of compound **2** was also analyzed. In these conditions, the most active catalysts were **2** and $[AlLiMe_2\{2,6\text{-}(MeO)_2C_6H_3O\}_2]_2$, with a conversion of 78% and 75% respectively. The activity of the heterometallic catalysts reduces when moving from Li to Na and K, with a conversion of 48% for **3b** and 20% for **3c**. For the most active catalysts, **2** and $[AlLiMe_2\{2,6\text{-}(MeO)_2C_6H_3O\}_2]_2$, the polymers obtained show narrow polydispersities,‡ especially when using the lithium–aluminium derivative. Further studies on these polymerization processes are underway.

Conclusions

A range of alkali metal $[AlMMe_2\{2,6\text{-}(MeO)_2C_6H_3O\}_2]_n$ derivatives have been isolated. In all the structures the presence of the $\{AlMe_2(2,6\text{-}(MeO)_2C_6H_3O)_2\}^-$ moiety is observed. This fragment could be described as a claw which fixes the alkali

---

‡ Compound **2**: M_n = 7951, polydispersity = 1.45; $[AlLiMe_2\{2,6\text{-}(MeO)_2C_6H_3O\}_2]_2$: M_n = 5653, polydispersity = 1.23.

metals by the phenoxide oxygen atoms while the methoxy groups help to stabilize the coordination sphere of these metals. When moving from Li to Na and K this aryloxide fragment does not change substantially the spectroscopic data or its structural parameters, only the dihedral angles between the central AlO_2 core and the phenyl rings modify to accommodate to the different alkali ions sizes. Preliminary polymerization studies indicate that the aluminium lithium species $[AlLiMe_2\{2,6\text{-}(MeO)_2C_6H_3O\}_2]_2$ are active in L-lactide ROP, giving polymers with narrower polydispersities than the homometallic counterpart **2**.

Acknowledgements

Financial support from Factoría de Cristalización-Consolider-Ingenio (CSD2006-00015) and the Universidad de Alcalá (CCG2013/EXP-061) are gratefully acknowledged. M. T. M. thanks the Universidad de Alcalá for a research fellowship. The authors thank Prof. Francisco Mendicuti and Thais Carmona for the CD measurements.

Notes and references

1 T. Taguchi and H. Yanai, Al(III) Lewis acids, in *Acid catalysis in modern organic synthesis*, ed. H. Yamamoto and K. Ishihara, Wiley, Weinheim, 2008; S. Woodward and S. Dagorne, *Modern Organoaluminum Reagents*, Springer, 2012; H. Naka, M. Uchiyama, Y. Matsumoto, A. E. H. Wheatley, M. McPartlin, J. V. Morey and Y. Kondo, *J. Am. Chem. Soc.*, 2007, **129**, 1921; H. Noth, A. Schlegel and M. Suter, *J. Organomet. Chem.*, 2001, **621**, 231; S. Saito and H. Yamamoto, *Chem. Commun.*, 1997, 1585.

2 J. Ternel, F. Agbossou-Niedercorn and R. M. Gauvin, *Dalton Trans.*, 2014, **43**, 4530; P. von Zezschwitz, *Synthesis*, 2008, 1809; Z. Elkhayat, I. Safir, M. Dakir and S. Arseniyadis, *Tetrahedron: Asymmetry*, 2007, **18**, 1589.

3 S. Baba and E.-I. Negishi, *J. Am. Chem. Soc.*, 1976, **98**, 6729; E.-i. Negishi and S. Baba, *J. Chem. Soc., Chem. Commun.*, 1976, 596.

4 U. M. Dezhemilev and V. A. D'yakonov, *Top. Organomet. Chem.*, 2013, **41**, 215; T. Miyoshi, S. Matsuya, M. Tsugawa, S. I. Sato, M. Ueda and O. Miyata, *Org. Lett.*, 2013, **15**, 3374.

5 O. Pamiés and M. Dieguez, *Top. Organomet. Chem.*, 2013, **41**, 277.

6 S. S. Kumar and H. W. Roesky, *Dalton Trans.*, 2004, 3927; P. von Zezschwitz, *Synthesis*, 2008, 1809; W. Uhl, *Coord. Chem. Rev.*, 2008, **252**, 1540; J. P. Campbell and W. L. Gladfelter, *Inorg. Chem.*, 1997, **36**, 4094.

7 E. Y. X. Chen and T. J. Marks, *Chem. Rev.*, 2000, **100**, 1391; H. Sinn and W. Kaminsky, *Adv. Organomet. Chem.*, 1980, **18**, 99; H. W. Roesky, M. G. Walawalkar and R. Murugavel, *Acc. Chem. Res.*, 2001, **34**, 201.

8 M. Miyamoto, Y. Saeki, H. Maeda and Y. Kimura, *J. Polym. Sci., Part A: Polym. Chem.*, 1999, **37**, 435; T. Kitayama, H. Yamaguchi, T. Kanzawa and T. Hirano, *Polym. Bull.*, 2000, **45**, 97; T. A. Zevaco, J. K. Sypien, A. Janssen, O. Walter and E. Dinjus, *J. Organomet. Chem.*, 2007, **692**, 1963; T. A. Zevaco, J. Sypien, A. Janssen, O. Walter and E. Dinjus, *Catal. Today*, 2006, **115**, 151.

9 M. Normand, T. Roisnel, J.-F. Carpentier and E. Kirillov, *Chem. Commun.*, 2013, **49**, 11692; O. Dechy-Cabaret, B. Martin-Vaca and D. Bourissou, *Chem. Rev.*, 2004, **104**, 6147; N. Spassky, M. Wisniewski, C. Pluta and A. Le Borgne, *Macromol. Chem. Phys.*, 1996, **197**, 2627; D. Commereuc, H. Olivier-Bourbigou, V. Kruger-Tissot and L. Saussine, *J. Mol. Catal. A: Chem.*, 2002, **186**, 215–222; M. O. Miranda, Y. DePorre, H. Vazquez-Lima, M. A. Johnson, D. J. Marell, C. J. Cramer and W. B. Tolman, *Inorg. Chem.*, 2013, **52**, 13692.

10 S. Dagorne and C. Fliedel, *Top. Organomet. Chem.*, 2013, **41**, 125; S. Milione, F. Grisi, R. Centore and A. Tuzi, *Organometallics*, 2006, **25**, 266–274; A. D. Schwarz, Z. Chu and P. Mountford, *Organometallics*, 2010, **29**, 1246–1260; M. H. Chisholm, C.-C. Lin, J. C. Gallucci and B.-T. Ko, *Dalton Trans.*, 2003, 406; M. Bouyahyi, T. Roisnel and J.-Fr. Carpentier, *Organometallics*, 2010, **29**, 491; B. J. O'Keefe, M. A. Hillmyer and W. B. Tolman, *Dalton Trans.*, 2001, 2215; A. Kowalski, A. Duda and S. Penczek, *Macromolecules*, 1998, **31**, 2114; P. Hormnirun, E. L. Marshall, V. C. Gibson, A. J. P. White and D. J. Williams, *J. Am. Chem. Soc.*, 2004, **126**, 2688; J. Liu, N. Iwasa and K. Nomura, *Dalton Trans.*, 2008, 3978; S. Dagorne, F. Le Bideau, R. Welter, S. Bellemin-Laponnaz and A. Maisse-François, *Chem. – Eur J.*, 2007, **13**, 3202; C. Zhang and Z.-X. Wang, *J. Organomet. Chem.*, 2008, **693**, 3151.

11 Y. Naganawa and K. Maruoka, *Top. Organomet. Chem.*, 2013, **41**, 187.

12 F. Mongin and A. Harrison-Marchand, *Chem. Rev.*, 2013, **113**, 7563; D. J. Linton, P. Schooler and A. E. H. Wheatley, *Coord. Chem. Rev.*, 2001, **223**, 53; R. E. Mulvey, D. R. Amstrong, B. Conway, E. Crosbie, A. R. Kennedy and S. D. Robertson, *Inorg. Chem.*, 2011, **50**, 12241.

13 R. E. Mulvey, *Dalton Trans.*, 2013, **42**, 6676; S. K. Mandal and H. W. Roesky, *Acc. Chem. Res.*, 2010, **43**, 248; R. E. Mulvey, *Organometallics*, 2006, **25**, 1060.

14 F. Soki, J.-M. Neudorfl and B. Goldfuss, *J. Organomet. Chem.*, 2008, **693**, 2139; W. Clegg, E. Lamb, S. T. Liddle, R. Snaith and A. E. H. Wheatley, *J. Organomet. Chem.*, 1999, **573**, 305; R. E. Mulvey, *Acc. Chem. Res.*, 2009, **42**, 743; H. R. Simmonds and D. S. Wright, *Chem. Commun.*, 2012, **48**, 8617.

15 J. García-Alvarez, E. Hevia, A. R. Kennedy, J. Klett and R. E. Mulvey, *Chem. Commun.*, 2007, 2402; R. E. Mulvey, F. Mongin, M. Uchiyama and Y. Kondo, *Angew. Chem., Int. Ed.*, 2007, **46**, 3802.

16 X. Pan, A. Liu, L. Yao, L. Wang, J. Zhang, J. Wu, X. Zhao and C.-C. Lin, *Inorg. Chem. Commun.*, 2011, **14**, 763; L. Wang, J. Zhang, L. Yao, N. Tang and J. Wu, *Inorg. Chem. Commun.*, 2011, **14**, 859; C. Decu, C. Casey, M. C. Case and

A. J. Shusterman, *Organometallics*, 2012, **31**, 7849; M. J. Harvey, M. Proffitt, P. Wei and D. A. Atwood, *Chem. Commun.*, 2001, 2094; S. Singh, J. Chai, A. Pal, V. Jancik, H. W. Roesky and R. Herbst-Irmer, *Chem. Commun.*, 2007, 4934; C. Gallegos, V. Tabernero, F. M. García-Valle, M. E. G. Mosquera, T. Cuenca and J. Cano, *Organometallics*, 2013, **32**, 6624.

17 V. Tabernero, M. E. G. Mosquera and T. Cuenca, *Organometallics*, 2010, **29**, 3642; G. Martínez, J. Chirinos, M. E. G. Mosquera, T. Cuenca and E. Gómez, *Eur. J. Inorg. Chem.*, 2010, 1522.

18 G. Martínez, S. Pedrosa, V. Tabernero, M. E. G. Mosquera and T. Cuenca, *Organometallics*, 2008, **27**, 2300.

19 M. T. Muñoz, C. Urbaneja, M. Temprado, M. E. G. Mosquera and T. Cuenca, *Chem. Commun.*, 2011, **47**, 11757.

20 L. Lochmann, J. Pospišil and D. Lim, *Tetrahedron Lett.*, 1966, **2**, 257.

21 R. H. Blessing, SORTAV, *Acta Crystallogr., Sect. A: Fundam. Crystallogr.*, 1995, **51**, 33.

22 L. J. Farrugia, *J. Appl. Crystallogr.*, 1999, **32**, 837.

23 G. M. Sheldrick, *Acta Crystallogr., Sect. A: Fundam. Crystallogr.*, 2008, **64**, 112.

24 P. Van der Sluis and A. L. Spek, *Acta Crystallogr., Sect. A: Fundam. Crystallogr.*, 1990, **46**, 194.

25 Search on the CSD, version 5.35 update Nov 2013.

26 D. Barr, W. Clegg, R. E. Mulvey, R. Snaith and K. Wade, *J. Chem. Soc., Chem. Commun.*, 1986, 295; D. R. Amstrong, D. Barr, W. Clegg, R. E. Mulvey, D. Reed, R. Snaith and K. Wade, *J. Chem. Soc., Chem. Commun.*, 1986, 869.

27 N. N. Greenwood and A. Earnshaw, *Chemistry of the Elements*, Pergamon, 1993, p. 86. Ionic radius (6-coordinate) Li 0.76 Å, Na 1.02 Å and K 1.38 Å.

28 G. A. Morris, *Diffusion-Ordered Spectroscopy, in Encyclopedia of Magnetic Resonance*, John Wiley & Sons, Ltd, UK, 2009; D. Li, I. Keresztes, R. Hopson and P. G. Williard, *Acc. Chem. Res.*, 2009, **42**, 270; D. R. Armstrong, P. García-Alvarez, A. R. Kennedy, R. E. Mulvey and J. A. Parkinson, *Angew. Chem., Int. Ed.*, 2010, **49**, 3185; S. E. Baillie, W. Clegg, P. Garcia-Alvarez, E. Hevia, A. R. Kennedy and L. Russo, *Chem. Commun.*, 2011, **47**, 388.

29 C. S. Barrett, *Acta Crystallogr.*, 1956, **9**, 671; A. Bondi, *J. Chem. Phys.*, 1964, **68**, 441.

30 A CSD search gave 17 hits for potassium polymeric structures with a K⋯K distance shorter than 3.6673 Å and 40 hits for dinuclear potassium derivatives.

31 J. A. Meese-Marktscheffel, R. Weimann, H. Schumann and J. W. Gilje, *Inorg. Chem.*, 1993, **32**, 5894; W. Uhl, A. Vester, D. Fenske and G. Baum, *J. Organomet. Chem.*, 1994, **464**, 23; A. Tapparo, S. L. Heath, P. A. Jordan, G. R. Moore and A. K. Powell, *J. Chem. Soc., Dalton Trans.*, 1996, 1601; W. Uhl, R. Gerding and A. Vester, *J. Organomet. Chem.*, 1996, **513**, 163; P. Henke, N. Trapp, C. E. Anson and H. Schnockel, *Angew. Chem., Int. Ed.*, 2010, **49**, 3146.

32 R. E. Mulvey, *Chem. Commun.*, 2001, 1049; D. R. Armstrong, E. Brammer, T. Cadenbach, E. Hevia and A. R. Kennedy, *Organometallics*, 2013, **32**, 480; S. E. Baillie, W. Clegg, P. García-Álvarez, E. Hevia, A. R. Kennedy, J. Klett and L. Russo, *Organometallics*, 2012, **31**, 5131.